

# Supplementary Material for HaLo-NeRF

SUBMISSION ID 1036

Landmark	Portal	Window	Spire	Tower	Dome	Minaret	#Seed	#Seg
NDC	✓	✓	✗	✓	✗	✗	15	4048
MC	✓	✓	✓	✗	✗	✗	19	902
SPC	✓	✓	✗	✓	✓	✗	20	731
BAM	✓	✗	✗	✗	✓	✓	15	177
BLM	✓	✓	✗	✗	✓	✓	26	381
HS	✓	✓	✗	✗	✓	✗	15	66

**Table 1: The HolyScenes Benchmark**, composed of the Notre-Dame Cathedral (NDC), Milan Cathedral (MC), St. Paul’s Cathedral (SPC), Badshahi Mosque (BAM), Blue Mosque (BLM), and the Hurva Synagogue (HS). Above we report the set of semantic categories annotated for each landmark, chosen according to their visible structure. In the columns on the right, we report the number of initial manually segmented images (#Seed), and the final number of ground-truth segmentations after augmented with filtered warps (#Seg)

## 1. HolyScenes – Additional Details

### 2 Landmarks and Categories Used.

Our benchmark spans three landmark building types (cathedrals, mosques, and a synagogue), from different areas around the world. We select scenes that have sufficient RGB imagery for reconstructing with [CZL\*22]. The images were taken from IMC-PT 20 [YI20] (*Notre-Dame Cathedral, St. Paul’s Cathedral*), MegaDepth [LS18] (*Blue Mosque*), WikiScenes [WAESS21] (*Milan Cathedral*), and scraped from Wikimedia Commons using the WikiScenes data scraping procedure (*Badshahi Mosque* and *Hurva Synagogue*). The Notre-Dame cathedral has the most images in the dataset (3,765 images), and the *Hurva Synagogue* has the fewest (104 images). For semantic categories, we select diverse concepts of different scales. Some of these (such as *portal*) are applicable to all landmarks in our dataset while others (such as *minaret*) only apply to certain landmarks. As illustrated in Table 1, we provide segmentations of 3-4 semantic categories for each landmark; these are selected based on the relevant categories in each case (e.g. only the two mosques have minarets).

### 20 Annotation Procedure

We produce ground-truth binary segmentation maps to evaluate our method using manual labelling combined with correspondence-guided propagation. We first segment 110 images from 3-4 different categories from each of the six different scenes in our dataset, as shown in Table 1. We then estimate homographies between these

26 images and the remaining images for these landmarks, using shared  
 27 keypoint correspondences from COLMAP [SF16] and RANSAC.  
 28 We require at least 100 corresponding keypoints that are RANSAC  
 29 inliers; we also filter out extreme (highly skewed or rotated) homo-  
 30 graphies by using the condition number of the first two columns of  
 31 the homography matrix. When multiple propagated masks can be  
 32 inferred for a target image, we calculate each pixel’s binary value  
 33 by a majority vote of the warped masks. Finally, we filter these aug-  
 34 mented masks by manual inspection. Out of 8,951 images, 6,195  
 35 were kept (along with the original manual seeds), resulting in a final  
 36 benchmark size of 6,305 items. Those that were filtered are mostly  
 37 due to occlusions and inaccurate warps. Annotation examples from  
 38 our benchmark are shown in Figure 1.

## 39 2. Implementation Details

### 40 2.1. Augmenting the WikiScenes Dataset

41 The original WikiScenes dataset is as described in Wu *et*  
 42 *al.* [WAESS21]. To produce training data for the offline stages  
 43 of our system (LLM-based semantic distillation and V&L model  
 44 semantic adaptation), we augment this cathedral-focused dataset  
 45 with mosques by using the same procedure to scrape freely-  
 46 available Wikimedia Commons collected from the root WikiCat-  
 47 egory “Mosques by year of completion”. The collected data con-  
 48 tains a number of duplicate samples, since the same image may  
 49 appear under different categories in Wikimedia Commons and is  
 50 thus retrieved multiple times by the scraping script. In order to de-  
 51 duPLICATE, we treat the image’s filename (as accessed on Wikime-  
 52 dia Commons) as a unique identifier. After de-duplication, we are  
 53 left with 69,085 cathedral images and 45,668 mosque images. Out  
 54 of these, we set aside the images from landmarks which occur in  
 55 HolyScenes (13,743 images total) to prevent test set leakage; the  
 56 remaining images serve as our training data.

### 57 2.2. LLM-Based Semantic Distillation

58 To distill the image metadata into concise textual pseudo-labels, we  
 59 use the instruction-tuned language model Flan-T5 [CHL\*22], se-  
 60 lecting the 3B parameter Flan-T5-XL variant. The model is given  
 61 the image caption, related key-words, and filename, and outputs a  
 62 single word describing a prominent architectural feature within the  
 63 image serving as its pseudo-label. Text is generated using beam  
 64 search decoding with four beams. The prompt given to Flan-T5 in-  
 65 cludes the instruction to *Write “unknown” if it is not specified* (i.e.  
 66 the architectural feature), in order to allow the language model to

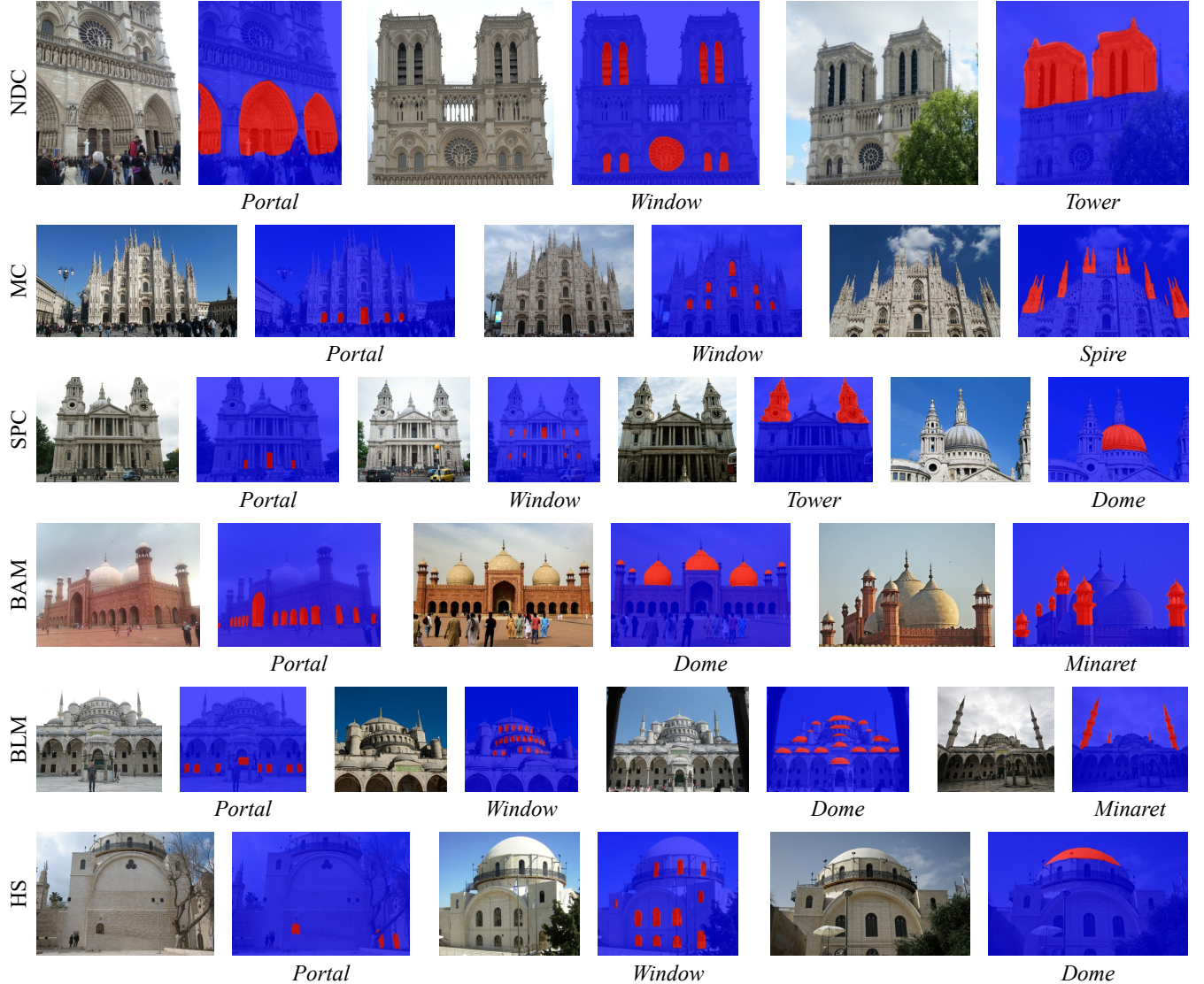


**Figure 1: HolyScenes annotations.** We illustrate annotations for each category in each landmark in the HolyScenes dataset: Notre-Dame Cathedral (NDC), Milan Cathedral (MC), St. Paul’s Cathedral (SPC), Badshahi Mosque (BAM), Blue Mosque (BLM), and Hurva Synagogue (HS).

67 express uncertainty instead of hallucinating incorrect answers in in-  
 68 determinate cases, as described in our main paper. We also find the  
 69 use of the building’s name in the prompt (*What architectural fea-*  
 70 *ture of <BUILDING>...*) to be important in order to cue the model to  
 71 omit the building’s name from its output (e.g. *towers of the Cathe-*  
 72 *dral of Seville* vs. simply *towers*).

73 To post-process these labels, we employ the following textual  
 74 cleanup techniques. We (1) employ lowercasing, (2) remove out-  
 75 puts starting with “un-” (“unknown”, “undefined” etc.), and (3) re-  
 76 move navigation words (e.g. “west” in “west facade”) since these  
 77 are not informative for learning visual semantics. Statistics on the  
 78 final pseudo-labels are given in Section 3.1.

### 79 2.3. Semantic Adaptation of V&L Models

80 We fine-tune CLIP<sub>FT</sub> on images and associated pseudo-labels, pre-  
 81 processing by removing all pairs whose pseudo-label begins with  
 82 “un-” (e.g. “unknown”, “undetermined”, etc.) and removing ini-  
 83 tial direction words (“north”, “southern”, “north eastern”, etc.), as  
 84 these are not visually informative. In total, this consists of 57,874  
 85 such pairs used as training data representing 4,031 unique pseudo-  
 86 label values; this includes 41,452 pairs from cathedrals and 16,422  
 87 pairs from mosques. Fine-tuning is performed on CLIP initialized  
 88 with the `clip-ViT-B-32` checkpoint as available in the  
 89 sentence-transformers model collection on Hugging Face  
 90 model hub, using the contrastive multiple negatives ranking loss as

91 implemented in the Sentence Transformers library. We train for 5  
 92 epochs with learning rate 1e-6 and batch size 128.

93 To collect training data based on image correspondences for  
 94 CLIPSeg<sub>FT</sub>, we use the following procedure: Firstly, to find pairs of  
 95 images in geometric correspondence, we perform a search on pairs  
 96 of images ( $I_1, I_2$ ) from each building in our train set along with  
 97 the pseudo-label  $P$  of the first image, applying LoFTR [SSW<sup>\*</sup>21]  
 98 to such pairs and filtering for pairs in correspondence where  $I_1$  is  
 99 a zoomed-in image corresponding to category  $P$  and  $I_2$  is a corre-  
 100 sponding zoomed-out image. We filter correspondences using the  
 101 following heuristic requirements:

- 102 • At least 50 corresponding keypoints that are inliers using  
 103 OpenCV’s USAC\_MAGSAC method for fundamental matrix cal-  
 104 culation.
- 105 • A log-ratio of at least 0.1 between the dispersion (mean square  
 106 distance from centroid, using relative distances to the image di-  
 107 mensions) of inlier keypoints in  $I_1$  and  $I_1$ .
- 108 • CLIP<sub>FT</sub> similarity of at least 0.2 between  $I_1$  and  $P$ , and at most  
 109 0.3 between  $I_2$  and  $P$ . This is because  $I_1$  should match  $P$ , while  
 110  $I_2$ , as a zoomed-out image, should contain  $P$  but not perfectly  
 111 match it as a concept.
- 112 • At least 3 inlier keypoints within the region  $R_P$  of  $I_1$  matching  $P$ .  
 113  $R_P$  is estimated by segmenting  $I_1$  with CLIPSeg and prompt  
 114  $P$  and binarizing with threshold 0.3.
- 115 • A low ratio of areas of the region matching  $P$  relative to the  
 116 building’s facade, since this suggests a localizable concept. This  
 117 is estimated as follows: We first find the quadrilateral  $Q$  which  
 118 is the region of  $I_2$  corresponding to  $I_1$ , by projecting  $I_1$  with  
 119 the homography estimated from corresponding keypoints. We  
 120 then find the facade of the building in  $I_2$  by segmenting  $I_2$  using  
 121 CLIPSeg with the prompt *cathedral* or *mosque* (as appropriate  
 122 for the given landmark), which outputs the matrix of probabili-  
 123 ties  $M$ . Finally, we calculate the sum of elements of  $M$  contained  
 124 in  $Q$  divided by the sum of all elements of  $M$ , and check if this  
 125 is less than 0.5.

126 Empirically, we find that these heuristics succeed in filtering out  
 127 many types of uninteresting image pairs and noise while select-  
 128 ing for the correspondences and pseudo-labels that are of interest.  
 129 Due to computational constraints, we limit our search to 50 images  
 130 from each landmark in our train set paired with every other image  
 131 from the same landmark, and this procedure yields 3,651 triplets  
 132 ( $I_1, I_2, P$ ) in total, covering 181 unique pseudo-label categories. To  
 133 use these correspondences as supervision for training segmenta-  
 134 tion, we segment  $I_1$  using CLIPSeg with prompt  $P$ , project this  
 135 segmentation onto  $I_2$  using the estimated homography, and using  
 136 the resulting segmentation map in the projected region as ground-  
 137 truth for segmenting  $I_2$  with  $P$ .

138 In addition to this data, we collect training data on a larger scale  
 139 by searching for images from the entire training dataset with crops  
 140 that are close to particular pseudo-labels. To do this, we run a search  
 141 by randomly selecting landmark  $L$  and one of its images  $I$ , se-  
 142 lecting a random pseudo-label  $P$  that appears with  $L$  (not necessar-  
 143 ily with the chosen image) in our dataset, selecting a random crop  
 144  $C$  of  $I$ , and checking its similarity to  $P$  with CLIP<sub>FT</sub>. We check if  
 145 the following heuristic conditions hold:

- 146 •  $C$  must have CLIP<sub>FT</sub> similarity of at least 0.2 with  $P$ .

- 147 •  $C$  must have higher CLIP<sub>FT</sub> similarity to  $P$  than  $I$  does.
- 148 • This similarity must be higher than the similarity between  $C$  and  
 149 the 20 most common pseudo-labels in our train dataset (exclud-  
 150 ing  $P$ , if it is one of these common pseudo-labels).
- 151 •  $C$  when segmented using CLIPSeg with prompt  $P$  must have  
 152 some output probability at least 0.1 in its central area (the central  
 153 280×280 region within the 352×352 output matrix).

154 If these conditions hold, we use the pair ( $I, P$ ) along with the  
 155 CLIPSeg segmentation of the crop  $C$  with prompt  $P$  as ground-truth  
 156 data for fine-tuning our segmentation model. Although this search  
 157 could be run indefinitely, we terminate it after collecting 29,440  
 158 items to use as training data.

159 For both sources of data (correspondence-based and crop-based),  
 160 we further refine the pseudo-labels by converting them to singular,  
 161 removing digits and additional direction words, and removing non-  
 162 localizable concepts and those referring to most of the landmark  
 163 or its entirety (“mosque”, “front”, “gothic”, “cathedral”, “side”,  
 164 “view”).

165 We fine-tune CLIPSeg to produce CLIPSeg<sub>FT</sub> by training for  
 166 10 epochs with learning rate 1e-4. We freeze CLIPSeg’s encoders  
 167 and only train its decoder module. To provide robustness to label  
 168 format, we randomly augment textual pseudo-labels by converting  
 169 them from singular to plural form (e.g. “window” → “windows”)  
 170 with probability 0.5. At each iteration, we calculate losses using a  
 171 single image and ground-truth pair from the correspondence-based  
 172 data, and a minibatch of four image and ground-truth pairs from the  
 173 crop-based data. We use four losses for training, summed together  
 174 with equal weighting, as described in Section ??.

175 CLIPSeg (and CLIPSeg<sub>FT</sub>) requires a square input tensor with  
 176 spatial dimensions 352×352. In order to handle images of vary-  
 177 ing aspect ratios during inference, we apply vertical replication  
 178 padding to short images, and to wide images we average predictions  
 179 applied to a horizontally sliding window. In the latter case, we use  
 180 overlapping windows with stride of 25 pixels, after resizing images  
 181 to have maximum dimension of size 500 pixels. Additionally, in  
 182 outdoor scenes, we apply inference after zooming in to the bound-  
 183 ing box of the building in question, in order to avoid attending to  
 184 irrelevant regions. The building is localized by applying CLIPSeg  
 185 with the zero-shot prompt *cathedral*, *mosque*, or *synagogue* (as ap-  
 186 propriate for the building in question), selecting the smallest bound-  
 187 ing box containing all pixels with predicted probabilities above 0.5,  
 188 and adding an additional 10% margin on all sides. While our model  
 189 may accept arbitrary text as input, we normalize inputs for metric  
 190 calculations to plural form (“portals”, “windows”, “spires” etc.) for  
 191 consistency.

## 192 2.4. 3D Localization

193 We build on top of the Ha-NeRF [CZL<sup>\*</sup>22] architecture with an  
 194 added semantic channel, similarly to Zhi *et al.* [ZLLD21]. This se-  
 195 mantic channel consists of an MLP with three hidden layers (di-  
 196 mensions 256, 256, 128) with ReLU activations, and a final output  
 197 layer for binary prediction with a softmax activation. We first train  
 198 the Ha-NeRF RGB model of a scene (learning rate 5e-4 for 250K it-  
 199 erations); we then freeze the shared MLP backbone of the RGB and

semantic channels and train only the semantic channel head (learning rate 5e-5, 12.5K iterations). We train with batch size 8,192. When training the semantic channel, the targets are binary segmentation masks produced by CLIPSeg<sub>FT</sub> with a given text prompt, using the inference method described above. We binarize these targets (threshold 0.2) to reduce variance stemming from outputs with low confidence, and we use a binary cross-entropy loss function when training on them.

For indoor scenes, we use all available images to train our model. For outdoor scenes, we select 150 views with segmentations for building the 3D semantic field by selecting for images with clear views of the building’s entire facade without occlusions. We find that this procedure yields comparable performance to using all the images in the collection, while being more computationally efficient. To select these images, we first segment each candidate image with CLIPSeg using one of the prompts *cathedral*, *mosque*, or *synagogue* (as relevant), select the largest connected component  $C$  of the output binary mask (using threshold 0.5), and sort the images by the minimum horizontal or vertical margin length of this component from the image’s borders. This prioritizes images where the building facade is fully visible and contained within the boundary of the visible image. To prevent occluded views of the building from being selected, we add a penalty using the proportion of overlap  $C$  and the similar binary mask  $C'$  calculated on the RGB NeRF reconstruction of the same view, since transient occlusions are not typically reconstructed by the RGB NeRF. In addition, we penalize images with less than 10% or more than 90% total area covered by  $C$ , since these often represent edge cases where the building is barely visible or not fully contained within the image. Written precisely, the scoring formula is given by  $s = m + c - x$ , where  $m$  is the aforementioned margin size (on a scale from 0 to 1),  $c$  is the proportion of area of  $C'$  overlapping  $C$ , and  $x$  is a penalty of 1.0 when  $C$  covers too little or much of the image (as described before) and 0 otherwise.

**Runtime.** A typical run (optimizing the volumetric probabilities for a single landmark) takes roughly 2 hours on a NVIDIA RTX A5000 with a single GPU. Optimizing the RGB and density values is only done once per landmark, and takes 2 days on average, depending on the number of images in the collection.

## 2.5. Baseline Comparisons

We provide additional details of our comparison to DFF [KMS22] and LERF [KKG\*23]. We train these models on the same images used to train our model. We use a Ha-NeRF backbone; similarly to our method we train the RGB NeRF representations for 250K steps and then the semantic representations for an additional 150K steps. Otherwise follow the original training and implementation details of these models, which we reproduce here for clarity.

For DFF, we implement feature layers as an MLP with 2 hidden layers of 128 and ReLU activations. The input to the DFF model is the images and the corresponding features derived from LSeg, and we minimize the difference between the learned features and LSeg features with an L2 loss, training with batch size 1024.

For LERF, we use the official implementation which uses the

Nerfacto method and the Nerfstudio API [TWN\*23]. The architecture includes a DINO MLP with one hidden layer of dimension 256 and a ReLU activation; and a CLIP MLP consisting of 3 hidden layers of dimension 256, ReLU activations, and a final 512-dimensional output layer. The input to this model consists of images, their CLIP embeddings in different scales, and their DINO features. We use the same loss as the original LERF paper: CLIP loss for the CLIP embeddings to maximize the cosine similarity, and MSE loss for the DINO features. The CLIP loss is multiplied by a factor of 0.01 similar to the LERF paper. We use an image pyramid from scale 0.05 to 0.5 in 7 steps. We train this model with batch size was 4096. We used also the relevancy score with the same canonical phrases as described in the LERF paper: “object”, “things”, “stuff”, and “texture”.

## 3. Additional Results and Ablations

### 3.1. Pseudo-Label Statistics

The pseudo-labels used in training consist of 4,031 unique non-empty values (over 58K images). The most common pseudo-labels are *facade* (5,380 occurrences), *dome* (3,084 occurrences), *stained class windows* (2,550 occurrences), *exterior* (2,365 occurrences), and *interior* (1,649 occurrences). 2,453 pseudo-labels occur only once (61% of unique values) and 3,426 occur at most five times (79% of unique values). Examples of pseudo-labels that only occur once include: *spiral relief*, *the attic*, *elevation and vault*, *archevêché*, *goose tower*, *pentcost cross*, *transept* and *croisée*.

We note the long tail of pseudo-labels includes items shown in our evaluation such as *tympanum* (29 occurrences), *roundel* (occurs once as *painted roundel*), *colonnade* (230 occurrences), and *pediment* (3 occurrences; 44 times as plural *pediments*).

### 3.2. CLIPSeg Visualizations

As described in our main paper, we leverage the ability of CLIPSeg to segment salient objects in zoomed-in images even when it lacks fine-grained understanding of the accompanying pseudo-label. To illustrate this, Figure 4 shows several results of inputting the target text prompt *door* to CLIPSeg along with images that do not have visible doors. As seen there, the model segments salient regions which bear some visual and semantic similarity to the provided text prompt (*i.e.* possibly recognizing an “opening” agnostic to its fine-grained categorization as a door, portal, window, etc). Our fine-tuning scheme leverages this capability to bootstrap segmentation knowledge in zoomed-out views by supervising over zoomed-in views where the salient region is known to correspond to its textual pseudo-label.

### 3.3. HaLo-NeRF Visualizations

In Figure 2, we compare segmentation results before and after 3D localization. We see that HaLo-NeRF exhibits 3D consistency, while 2D segmentation results of CLIPSeg<sub>FT</sub> operating on each image separately exhibit inconsistent results between views. We also see that this effect is prominent when using these methods for binary segmentation, obtained by thresholding predictions.

In Figure 3, we demonstrate our ability to perform localization

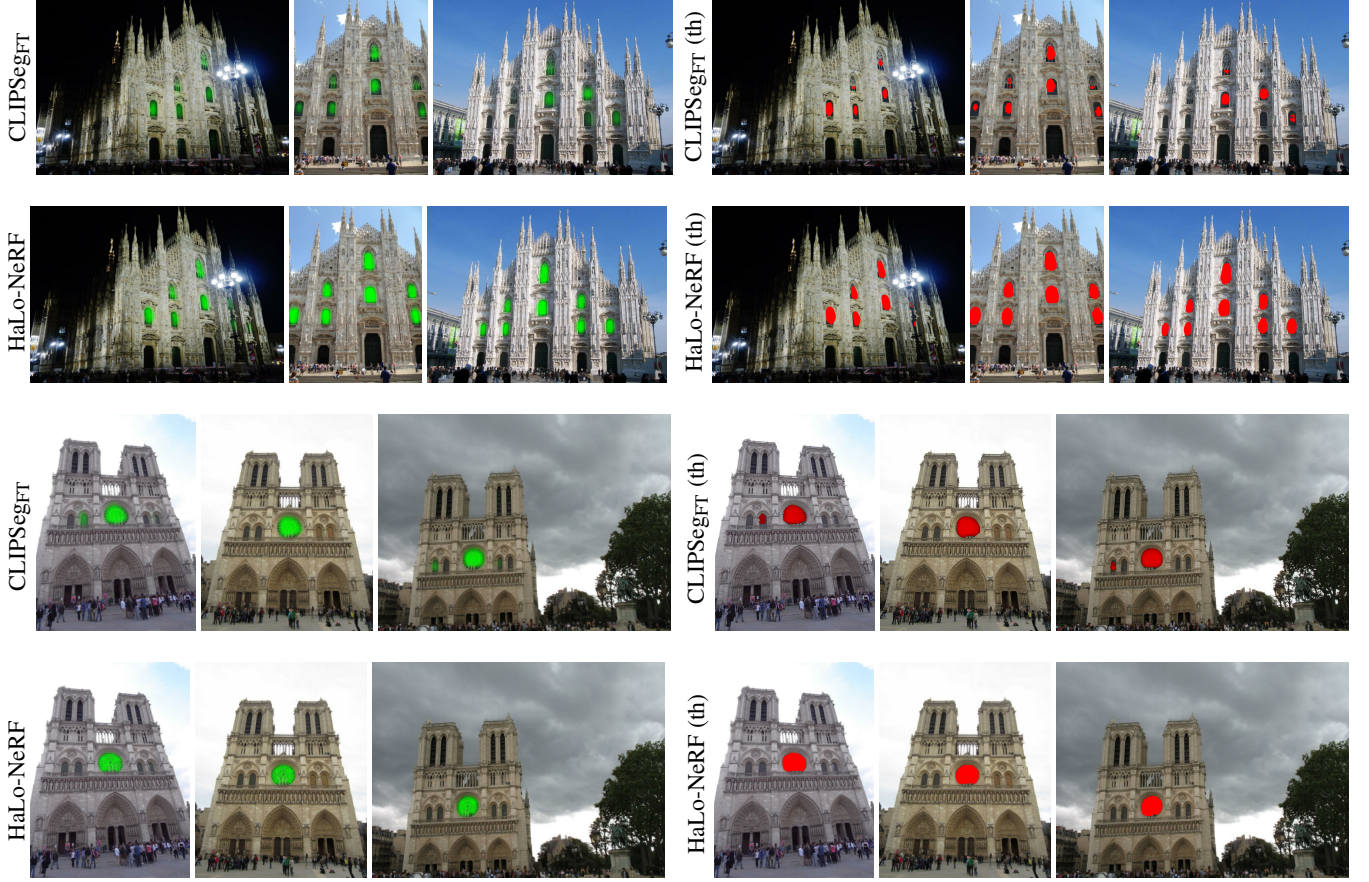


**Figure 2: Results before and after 3D localization.** Segmentation results for the prompts windows and rose window are presented in the first and last pairs of rows, respectively. We show the results of CLIPSegFT and HaLo-NeRF’s projected localization in green, observing that HaLo-NeRF yields 3D-consistent results by fusing the 2D predictions of CLIPSegFT, which exhibit view inconsistencies. We also show binary segmentation (th) obtained with threshold 0.5 in red, seeing that inconsistencies are prominent when using these methods for binary prediction.

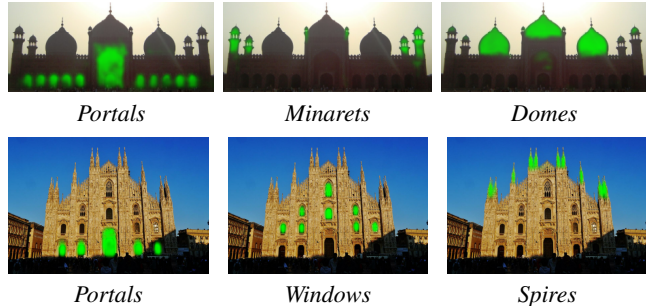


**Figure 3: Different localization images for the same scene.** We show multiple semantic concept localizations of HaLo-NeRF for a single scene view. These results on Badshahi Mosque (first row) and Milan Cathedral (second row) illustrate how the user may provide HaLo-NeRF with multiple text prompts to understand the semantic decomposition of a scene.

of multiple semantic concepts in a single view of a scene. By providing HaLo-NeRF with different text prompts, the user may decompose a scene into semantic regions to gain an understanding of its composition.

#### 3.4. 2D Baseline Visualizations

In Figure 5, we visualize outputs of the two 2D baseline segmentation methods (LSeg and ToB) as well as CLIPSeg and our fine-tuned CLIPSegFT. We see that the baseline methods struggle to attend to the relevant regions in our images, while CLIPSegFT shows the best understanding of these concepts and their localizations.

#### References

- [CHL<sup>\*</sup>22] CHUNG H. W., HOU L., LONGPRE S., ZOPH B., TAY Y., FEDUS W., LI E., WANG X., DEHGHANI M., BRAHMA S., ET AL.: Scaling Instruction-Finetuned Language Models. *arXiv preprint arXiv:2210.11416* (2022).

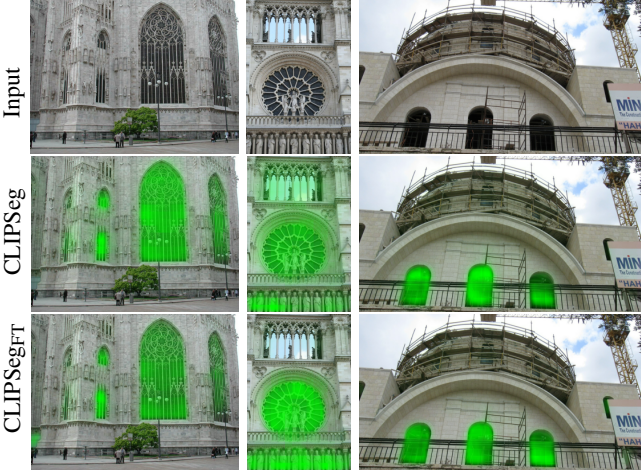


**Figure 4: Providing text-based segmentation models with partially related text prompts.** Above we provide the target prompt *door* to CLIPSeg (pretrained and fine-tuned) along with images that do not have visible doors. As seen above, the models instead segment more salient regions which bear some visual and semantic similarity to the provided text prompt (in this case, segmenting windows).

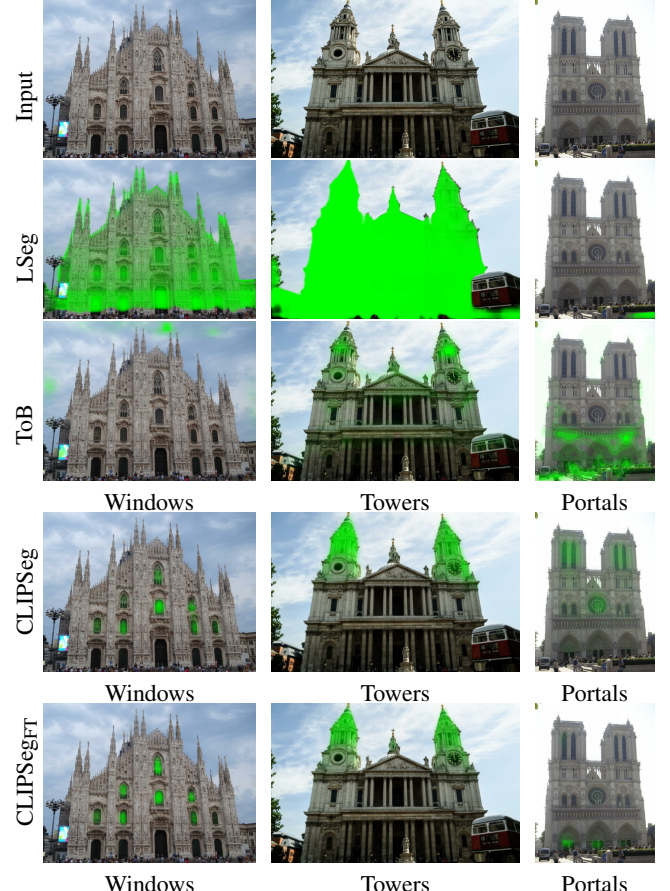


**Figure 5: Illustration of baseline 2D segmentation methods.** As is seen above, the baseline methods (LSeg and ToB) struggle to attend to the relevant regions in the images, while CLIPSegFT shows the best understanding of these concepts and their localizations, consistent with our quantitative evaluation.

- 319 [CZL\*22] CHEN X., ZHANG Q., LI X., CHEN Y., FENG Y., WANG X.,  
320 WANG J.: Hallucinated Neural Radiance Fields in the Wild. In *Proceedings of the IEEE/CVF Conference on Computer Vision and Pattern  
321 Recognition (CVPR)* (2022), pp. 12943–12952. 1, 3
- 322 [KKG\*23] KERR J., KIM C. M., GOLDBERG K., KANAZAWA A., TAN-  
323 CIK M.: Lerf: Language embedded radiance fields. *arXiv preprint arXiv:2303.09553* (2023). 4
- 324 [KMS22] KOBAYASHI S., MATSUMOTO E., SITZMANN V.: Decompos-  
325 ing NeRF for Editing via Feature Field Distillation. In *Advances in Neu-  
326 ral Information Processing Systems (NeurIPS)* (2022). 4
- 327 [LS18] LI Z., SNAVELY N.: Megadepth: Learning single-view depth pre-  
328 diction from internet photos. In *Proceedings of the IEEE conference on computer vision and pattern recognition* (2018), pp. 2041–2050. 1
- 329 [SF16] SCHONBERGER J. L., FRAHM J.-M.: Structure-from-motion re-  
330 visited. In *Proceedings of the IEEE conference on computer vision and  
331 pattern recognition* (2016), pp. 4104–4113. 1
- 332 [SSW\*21] SUN J., SHEN Z., WANG Y., BAO H., ZHOU X.: Loftr:  
333 Detector-free local feature matching with transformers. In *Proceedings  
334 of the IEEE/CVF conference on computer vision and pattern recognition* (2021), pp. 8922–8931. 3
- 335 [TWN\*23] TANCIK M., WEBER E., NG E., LI R., YI B., KERR J.,  
336 WANG T., KRISTOFFERSEN A., AUSTIN J., SALAHI K., ET AL.: Nerf-  
337 studio: A modular framework for neural radiance field development.  
338 *arXiv preprint arXiv:2302.04264* (2023). 4
- 339 [WAESS21] WU X., AVERBUCH-ELOR H., SUN J., SNAVELY N.: Tow-  
340 ers of Babel: Combining Images, Language, and 3D Geometry for Learn-  
341 ing Multimodal Vision. In *Proceedings of the IEEE/CVF International  
342 Conference on Computer Vision (ICCV)* (2021), pp. 428–437. 1
- 343 [Yi20] YI K. M.: Image matching: Local features & beyond  
344 2020. <https://www.cs.ubc.ca/~kmyi/imw2020/data.html>, 2020.  
345 <https://www.cs.ubc.ca/~kmyi/imw2020/data.html>. URL: <https://www.cs.ubc.ca/~kmyi/imw2020/data.html>, arXiv:  
346 <https://www.cs.ubc.ca/~kmyi/imw2020/data.html>. 1
- 347 [ZLLD21] ZHI S., LAIDLLOW T., LEUTENECKER S., DAVISON A. J.:  
348  
349  
350  
351  
352

In-Place Scene Labelling and Understanding with Implicit Scene Representation. In *Proceedings of the IEEE/CVF International Conference on Computer Vision (CVPR)* (2021), pp. 15838–15847. 3